Species-specific loss of genetic diversity and accumulation of genetic load following agricultural intensification

Zachary J. Nolen[1*], Patrycja Jamelska[1,2], Ana Sofia Torres Lara[1,3], Niklas Wahlberg[1], Anna Runemark[1]

[1] Department of Biology, Lund University, Lund, Sweden 22362

[2] Institute of Biology, University of Neuchâtel, Neuchâtel, Switzerland 2000

[3] Faculty 2 Biology/Chemistry, University of Bremen, Bremen, Germany 28359

* Corresponding author: Zachary J. Nolen; Kontaktvägen 10, Lund 22362, Sweden; zachary.nolen@biol.lu.se

Keywords: Conservation, agricultural intensification, inbreeding, genetic load, genomic erosion, historical DNA

Abstract

Agriculture driven land-use change is a major contributor to insect declines globally. As a result of population decline and subdivision, species lose genetic diversity, potentially reducing adaptive potential and increasing genetic load, reinforcing decline. We examine how genetic diversity has changed over the past century in three Polyommatinae (Lepidoptera: Lycaenidae) butterfly species in southern Sweden, leveraging genome sequencing of specimens from museum collections. Based on 63 historical and 92 contemporary genomes, we document a general decline in genetic diversity and reveal that the extent of decline depends on habitat specialization. The habitat generalist has retained most of its genetic diversity and connectivity. In contrast, the two specialists have declined sufficiently that even common variation is being eroded by drift, with up to a 3.3% reduction in heterozygosity per decade in the strongly grassland associated *Cyaniris semiargus*. While this sharp decline has reduced total genetic load in the two specialist species, increased population isolation has led to inbreeding in *Cy. semiargus*, exposing a greater proportion of load in homozygous state. This realized load likely reduces mean fitness and reinforces population decline, highlighting the need for well-connected grassland landscapes to maintain grassland specialist functional connectivity and genetic diversity. We complement these analyses with data on seven additional Polyommatinae species, uncovering that declines are common across the group, with alarming rates of genetic decline in species listed as viable. This study highlights the urgency of incorporating genetic data into conservation planning, as threats from genetic erosion are not captured by current conservation assessment.

Introduction

Insect decline has received increased attention in recent years as reports uncover alarming declines in insect assemblages and biomass (1). Efforts to quantify this decline estimate that terrestrial insects are declining at an average rate of 11% per decade globally, with this trend being primarily driven by even stronger regional declines in Europe and North America (2). This stark decline is the result of a variety of anthropogenic pressures, primarily climate change and land use changes such as agricultural intensification and urbanization (1, 3–7). Intensive agricultural landscapes place a particularly strong pressure on grassland insect species (6), especially in Europe where formerly biodiverse semi-natural grasslands have been abandoned or converted into intensively cultivated land (8).

While these declines already have alarming implications for natural communities and ecosystem services in which insects play key roles, they can also leave insect populations with genetic challenges to long term persistence. Declining populations are expected to lose genetic diversity as the relative strength of genetic drift increases, reducing their ability to adapt to changing environments and potentially unmasking genetic load through inbreeding and weakened selection (9). These processes can reduce mean fitness within the population, reinforcing demographic decline, a process referred to as mutational meltdown (10). An increasing number of studies document that this process can continue even upon demographic recovery, with persisting loss of genetic diversity and accumulation of genetic load due to drift debt (11–14).

How to assess the threat genetic factors pose to natural populations is still an active area of research, with several genetic monitoring approaches being suggested and implemented (15–18). Interpretation of genetic diversity is complex, as it is influenced by a multitude of factors (19), such as ecology and life history (20), genomic architecture (21), and demographic trends over thousands to millions of years (22). Low genetic diversity is thus not always a cause for alarm, as populations with a long history of small population sizes may have effectively purged deleterious variation that threatens persistence (23–25). Rather, reductions in genetic diversity in historically

large populations, which carry a high masked potential load, can increase extinction risk as genetic load becomes stochastically realized (9, 26).

The rate of genetic decline, rather than current levels of genetic diversity, has become a focus for genetic monitoring, with programs in several countries using genetic metrics measured over time or that can directly measure ongoing genetic decline (16, 27), e.g. contemporary effective population size (28). Temporal sampling is, however, limited to estimating genetic decline from the first sampled time point, with considerable erosion likely to have occurred several decades before. To overcome this, genomic resources from historic samples preserved in natural history museums can be an invaluable resource, extending monitoring further back in time. The direct measures of pre- and early bottleneck genetic parameters museum samples provide are crucial to fully understand the extent and character of genetic decline (18).

Here, we use museomics to address to what extent genetic diversity has been lost and functional connectivity reduced in grassland associated butterflies during the second wave of agricultural modernization in Sweden starting in the 1940s (29, 30). During this modernization, small farms were abandoned and their associated semi-natural grasslands began to decline considerably (30). We examine three focal butterfly species in this landscape that vary in habitat specialization, ranging from grassland generalist to specialist, enabling us to examine if patterns of genetic decline are stronger in more specialized species, in line with expectations from greater demographic declines in specialist insect abundance compared to generalists (31–33). By comparing pairs of historical population samples collected in southern Sweden in the early 20th century with their contemporary counterparts, we document species-specific losses of genetic diversity and functional connectivity, as well as increased inbreeding depression in the most specialized species. We further examine if patterns of loss of genetic diversity are general, and if loss of genetic diversity is reflected in current conservation status, by extending the dataset to include historical and modern individuals of seven additional related butterfly species with Swedish Red List (34) conservation statuses ranging from least concern to critically endangered.

Results

We analyzed changes in genetic diversity, differentiation, and genetic load in three focal Polyommatinae (Lepidoptera: Lycaenidae) butterfly species: *Polyommatus icarus,* a grassland generalist, *Plebejus argus*, a heathland specialist, and *Cyaniris semiargus*, a grassland specialist (Figure 1A). We generated whole genome resequencing data from pinned museum specimens from the entomological collections of the Biological Museum at Lund University (35) collected from 1917-1956 (Table S1; *N* = 28 - *Po. icarus*; 12 - *Pl. argus*; 14 - *Cy. semiargus*) in Southern Sweden. These individuals were sampled in populations generally collected at the same locality during the same year, and compared with WGS data from samples collected at corresponding localities in 2020-2023 by Nolen et al (36) (Figure 1B; Table S1; *N* = 27 - *Po. icarus*; 29 - *Pl. argus*; 29 - *Cy. semiargus*). As DNA extracted from historical specimens is fragmented and subject to post-mortem DNA damage (37, 38) (Figure S1), we confirmed shorter fragments did not induce a reference bias in the historical samples (Figure S2). To address DNA damage, we tested post-mortem DNA damage correction I) using MapDamage2 (39) and II) removing all transition sites, which are the most common changes caused by DNA damage (37, 38). Rescaling base quality scores with MapDamage2 biased historical samples towards the reference in two of the three focal species, whereas transition removal did not (Figure S2). All subsequent results were therefore generated without MapDamage2 correction and with transitions removed. To account for lower sequencing depth in historical samples, we performed analyses both at full depth and with samples subsampled to equivalent mean sequencing depths, presenting the subsampled results in the main text, with full depth results included in the Appendix.

General reductions in genetic diversity

To assess if agricultural intensification and the associated reduction in semi-natural grassland habitat has resulted in reduced genetic diversity, we compared individual genome-wide heterozygosity of historical and modern samples within each species. In all three species, heterozygosity is lower in modern individuals, but considerably more so in the two specialist species compared to the generalist (Welch two-sample t-test: $P = 0.006$ in *Po. icarus*, < 0.001 in *Pl. argus*, and < 0.001 in *Cy. semiargus;* Figure 1C;

Tables S2-3). In the specialist species, *Pl. argus* and *Cy. semiargus*, population-specific estimates of genetic diversity are lower in all modern populations compared to their historical counterparts, both for nucleotide diversity (π; Wilcoxon signed-rank test: median effect size range [-0.52, -0.40] in *Pl. argus* and [-0.76, -0.51] in *Cy. semiargus*) and Watterson's θ (median effect size range [-0.77, -0.68] in *Pl. argus* and [-0.86, 0.70] in *Cy. semiargus*), even after subsampling to account for variation in sample size (Figure S3; Tables S4-5). In the generalist, *Po. icarus*, only Watterson's θ shows declines robust to variation in sample size, and only in two of the three populations (median effect size range [-0.29, -0.24]; Figure S3; Table S4-5). Tajima's D is higher in modern populations of all three species compared to their historical counterparts, consistent with population bottlenecks across the past century (median effect size range [0.63, 0.68] in *Po. icarus*, [0.82, 0.84] in *Pl. argus*, and [0.73, 0.85] in *Cy. semiargus*; Figure S3; Table S4-5).

Reduced connectivity may accelerate loss of genetic diversity

While genetic diversity decline is an expected product of demographic decline, it can additionally be accelerated by reductions in gene flow (40). We reveal a loss of functional connectivity among modern populations, reflected in stronger contemporary population structure, supported by both genetic differentiation and clustering approaches, likely contributing to the loss of genetic diversity. *Po. icarus* and *Cy. semiargus* have stronger genetic differentiation (F_{ST}) between modern than historical population pairs (Paired t-test: $\Delta F_{ST} = 0.014$, $P = 0.007$ in *Po. icarus* and $\Delta F_{ST} = 0.053$, $P = 0.036$ in *Cy. semiargus*; Figure 1F; Table 6-7). F_{ST} increased in *Pl. argus* in the single population pair present in both time periods ($\Delta F_{ST} = 0.021$; Table S7). Including all modern population pairs in the analysis estimates mean F_{ST} increases of 0.027 and 0.071 in *Pl. argus* and *Cy. semiargus*, respectively (Welch two-sample t-test: $P = 0.001$ in *Cy. semiargus*;Table S7). Principal component analyses (PCAs) and admixture analyses also reveal generally stronger population structure in modern samples than historical, and strongest in the most specialized *Cy. semiargus* (Figure 2A). Along PC1, the greatest axis of variation, both *Po. icarus* and *Pl. argus* are clustered primarily into historical and modern samples, consistent with the best fit admixture analyses for these

species (K=2; Figure 2B; Table S8). In these two species, modern samples show greater among population differences than historical along PC2, however, consistent with increases in genetic differentiation between localities. Greater than two clusters are visible on the PCA for these two species, which, along with the correlation of residuals for the admixture analyses (Figure S4), highlights that greater genetic structure likely exists in these two species, but from low enough variation that we cannot reliably uncover it with our sample sizes. Each modern population forms a distinct cluster in the specialized species, *Cy. semiargus*, while historical populations cluster together in their own separate cluster (Figure 2B). The stronger contemporary population structure is especially driven by isolation of populations in the agricultural landscapes within Sweden's southernmost province, Skåne (Figure 1D; Figure 2B; Figure S5).

Species-specific increases in inbreeding

The pronounced losses of functional connectivity and genetic diversity have resulted in inbreeding within the specialist *Cy. semiargus*. This contemporary inbreeding is reflected by an increase in the inbreeding coefficient F_{RoH} from historical to modern *Cy. semiargus* samples (Welch two-sample t-test: $\Delta F_{RoH} = 0.065$, $P < 0.001$; Figure 1D; Table S3&9). F_{RoH} measures the proportion of the autosomal genome in runs of homozygosity greater than a certain length (41), which we set to 100kb, roughly corresponding to identical by descent tracks with shared ancestry in the past 200 generations (42). Across species, no historical individual has a coefficient greater than 0.04, and historical species averages are all below 0.01. In *Cy. semiargus*, modern samples have a maximum coefficient of 0.33 and an average coefficient of 0.072, an order of magnitude higher than the mean for historical samples. In modern *Cy. semiargus*, individuals with higher inbreeding coefficients have fewer runs of homozygosity relative to their cumulative length, which may indicate they stem from close-kin matings (Figure 3A, Figure S6). For other individuals, there is a largely linear relationship between the number of runs of homozygosity and their cumulative length, suggesting that close-kin mating is not common overall and inbreeding is primarily due to increases in background relatedness, consistent with patterns expected of a population bottleneck (42).

Purging of total genetic load

Population decline and subdivision can result in increased exposure of genetic load, in the form of rare recessive deleterious variants in a homozygous state, to selection (43). This may facilitate purging, but can also result in greater realization of minorly deleterious variation in homozygous state, reducing mean population fitness and reinforcing decline. We find evidence consistent with purging in both specialist species *Pl. argus* and *Cy. semiargus*, as total genetic load is lower in modern compared to historical samples both for high (e.g. loss of function; Welch two-sample t-test: P = 0.024 in *Pl. argus* and 0.021 in *Cy. semiargus*) and moderate (e.g. missense; $P < 0.001$ in *Pl. argus* and = 0.003 in *Cy. semiargus*) impact variants (Figure 3B; Table S10). In generalist *Po. icarus*, total genetic load from high and moderate impact variants is similar in modern and historical samples. Total genetic load from derived variants at highly genomically conserved positions has remained stable in all three species.

Increased realized genetic load in *Cy. semiargus*

Modern individuals have greater realized genetic load at moderate impact sites compared to historical individuals in *Cy. semiargus* (P = 0.013; Figure 3C; Table S10), despite evidence for purging of the genetic load in this species. In contrast, there is no increase in realized load for high impact sites. Realized genetic load incorporates only putatively deleterious alleles in a homozygous state, reflecting the proportion of total load that is expressed in an individual. We find no evidence for increases in realized genetic load at moderate or high impact sites in *Po. icarus* or *Pl. argus*, with realized load even decreasing at moderate sites in *Pl. argus* ($P < 0.001$; Figure 3C; Table S10). However, derived variants at conserved regions are realized to a greater extent in modern samples of both *Pl. argus* and *Cy. semiargus* ($P < 0.001$ in *Pl. argus* and = 0.009 in *Cy. semiargus*; Figure 3C; Table S10), despite total load in these regions remaining stable. In *Cy. semiargus*, individuals with higher inbreeding coefficients had higher realized, but not total, genetic load across all variant categories (linear regression: R^2 = 0.46, 0.37, 0.77 for conserved, high, and moderate impact variants, respectively; Figure S7), indicative of inbreeding depression.

Genetic decline not reflected in current conservation status

We utilized the genetic decline indicator thresholds outlined by Andersson et al (15) to determine if current conservation status relates to the rate of genetic decline. These thresholds suggest categorizations of ‘Acceptable’, ‘Warning’, and ‘Alarm’ rates of genetic decline, reflecting >=95%, 75-94%, and <75% retention of genetic diversity over 100 years, respectively. Based on changes in heterozygosity, nucleotide diversity, and Watterson’s θ, *Po. icarus* largely exhibits ‘Acceptable’ or ‘Warning’ declines, while *Pl. argus* and *Cy. semiargus* exhibit ‘Warning’ or ‘Alarm’ declines, depending on the metric of genetic diversity used (Figure 4&S8; Tables S5&11), which largely are in line with the concerns raised by our genetic load analyses. This is in stark contrast with the 2020 Swedish Red List of species (34), where all three focal species share a conservation status of ‘Least Concern’.

To assess if the loss of genetic diversity in the three focal species is representative of other grassland butterfly species, we supplemented the dataset by generating whole genome resequencing data for historical-modern pairs of seven additional species of Polyommatinae butterfly (Table S1). We assessed if the conservation status of these species, ranging from of ‘Least Concern’ to ‘Critically Endangered’ (34) (Table S12) capture losses of genetic diversity uncovered in this data set. Comparing individual heterozygosity, we find that current conservation status generally fails to capture the levels of genetic erosion in these species (Figure 4A&S8; Table S11). Utilizing estimates at full individual sequencing depth, least concern species predominantly fell into the warning category, with only *Celastrina argiolus* and Öland *Po. icarus* falling in the acceptable category. Of species classified as least concern, only *Cy. semiargus* fell into the alarm category. Two endangered species, *Phengaris alcon* and *Scolitantides orion,* fell into the acceptable and alarm categories, respectively, with *Ph. alcon* even increasing slightly in genetic diversity over the time frame. *Plebejus argyrognomon*, a critically endangered species that is now presumed extinct in Sweden (44), had already experienced genetic decline categorized as ‘alarm’ by the early 2000s, when our modern sample for this species was collected. Results from our focal species illustrate that categorization can depend considerably on the individuals/populations sampled

(Figure 4). Categorization is largely consistent for each species both at full sequencing depth and when subsampled to 2-3X sequencing depth, but some species/populations bordering adjacent categories shift between them upon subsampling (Table S11).

Discussion

Our analyses of 63 historical and 92 modern genomes uncover a decline in butterfly genetic diversity over the past century. This decline is greater in the specialist species, especially *Cy. semiargus*, where the once highly connected populations have become isolated into distinct genetic clusters. This subdivision and resulting loss of diversity has increased rates of inbreeding and exposed genetic load to natural selection, resulting in purging of both high and moderate impact mutations. Importantly, we uncover a higher realization of genetic load in conserved regions and at moderate impact variants in modern *Cy. semiargus*, likely reducing fitness. The rates of decline uncovered in the three focal species examined are also common in seven additional species of blue butterflies, despite most of these species having conservation statuses of 'Least Concern'. Our findings reveal that recent genetic erosion is likely to be ubiquitous across grassland butterflies in southern Sweden. These results highlight the need for incorporation of genetic data into conservation assessments of insect threat status, as census-based estimates fail to detect threats posed by genetic decline.

Our findings of reduced genetic diversity across all three focal species are consistent with widespread demographic decline in arthropod species in Europe over the past century, with the modernization of agriculture as a major driver (5, 45). The highest average decline in genetic diversity we document, an up to 3.3% reduction in heterozygosity per decade in *Cy. semiargus,* appears to be accelerated by strengthened isolation between populations. However, both *Po. icarus* and *Pl. argus*, where increases in population subdivision are more moderate, have experienced declines of up to 0.7% and 2.7% per decade, respectively. Population structure and genetic differentiation analyses suggest modest increases in population isolation in these species, potentially reflecting that declines in genetic diversity predate genomic signals of population subdivision. Population differentiation accumulates over time, lagging behind barriers to gene flow (46, 47), with the rate at which genetic

differentiation accumulates after subdivision depending upon the underlying effective population sizes of the populations (48).

Importantly, the finding that these three species have historically had low levels of genetic differentiation across southern Sweden highlights that currently isolated populations may be made up of partitions of historically well-connected metapopulations. Hence, concerns about genetic rescue (49) wiping out locally adapted ancestry (50, 51) are not likely to be relevant for these and other grassland associated insects in regions with historically abundant habitat. Instead, restoring functional connectivity to reduce inbreeding and associated accumulation of deleterious genetic variation (10, 52) is likely key to improve prospects of long-term persistence. Previous work on *Cy. semiargus* has shown that the inbreeding in these modern populations is related to low grassland land cover in the surrounding landscape (36). Expanding green infrastructure and restoration of semi-natural grassland habitat, enabling dispersal and buffering genetic decline, is likely needed to remedy future isolation and inbreeding in grassland associated butterflies.

Understanding to what extent genetic diversity decline actually reduces the fitness of individuals and populations is crucial for determining conservation priorities. The relationship between genetic diversity and extinction risk is highly contextual, and may be confounded by demography and dispersal dynamics (25). To determine if extinction risk has increased without having direct estimates of fitness, we assess genetic load. Decreases in genetic load may reflect purging of recessive, highly deleterious variation during and after a bottleneck, as the increased strength of genetic drift and higher rates of inbreeding expose recessive variants to selection in homozygous state (43). However, while selection may be strong enough to purge highly deleterious alleles, moderately deleterious alleles may become expressed more often due to increased homozygosity, with insufficient selective pressure to overcome the increased strength of drift (9, 26, 53). We reveal that both specialist species have experienced purging of both loss of function and missense mutations. Despite this, in *Cy. semiargus*, increases in inbreeding have led to higher realized genetic load from persisting missense mutations, largely driven by greater expression of load in individuals with higher inbreeding

coefficients. Reduced heterozygosity has been shown to increase extinction risk in small, isolated, recently declined populations belonging to a larger meta-population of the Glanville fritillary butterfly (*Melitaea cinxia*) (25, 54), underscoring the risks associated with increased expression of genetic load in the recently isolated, inbred populations of *Cy. semiargus*.

Genetic load estimates must be interpreted with consideration. Functional effect based genetic load estimates are reliant upon correct underlying gene models in the annotation and assume the reference allele is less deleterious than the alternate. We define conserved positions by selecting those with the top 1% of Genomic Evolutionary Rate Profiling (GERP) scores, however, these scores may not confidently distinguish between weakly and strongly deleterious mutations (55, 56). Our score thresholds are notably lower than thresholds utilized to assess genetic load in vertebrates (55, 57–59), and lower than estimates for other Lepidopterans estimated from a multi-species alignment (60), the latter likely due to our use of a time tree to estimate scores compared to a neutral rate tree by Bortoluzzi et al (60). However, our identification of conserved sites should be robust for within-species genetic load comparisons, as they represent the upper extreme of the distribution in our data. Moreover, our findings are consistent with predictions from population genetic theory, and hence likely reflect true impacts on genetic load and can inform management for these species. Genetics informed conservation action to increase long-term viability must focus on reducing both masked and realized genetic load (26). This is most pressing in *Cy. semiargus*, where translocations are likely necessary if populations with high levels of inbreeding are not to suffer continued decline from inbreeding depression.

None of the three focal species are currently demographically declining at a rate to qualify for the Swedish Red List based on demographic data. Systematic monitoring in Sweden from 2010-2023 reveal declines in both *Po. icarus* and *Cy. semiargus*, while *Pl. argus* appears to have stabilized (61). Demographic stability in *Pl. argus* does not necessarily mean that genetic diversity has stabilized in the species, as populations may continue to lose genetic diversity even after demographic recovery, a phenomenon termed drift debt (11). In *Cy. semiargus*, genetic factors are likely already contributing to

its demographic decline. Our findings illustrate the importance of incorporating genetic monitoring into conservation assessment (62, 63) to identify genetic decline before it results in expressed genetic load. Temporal monitoring with historical samples provides an opportunity to detect species facing recent declines in genetic diversity, separating them from those with longer term low genetic diversity (18). Using this approach on several species of Polyommatinae blues in southern Sweden, we document a general loss of genetic diversity in grassland butterflies and uncover that additional species currently not on the Red List likely face threats from reduced genetic diversity. Estimations of genetic decline along with complementary estimates of genetic load provide a promising way to assess genetic conservation concerns in the wild (14), but these analyses are limited by the availability of high quality reference genomes. This underscores the importance of efforts to generate high quality references for wild species, as they will improve our ability to accurately assess these metrics (64).

In conclusion, we document a general decline in genetic diversity in grassland butterflies in southern Sweden, which is likely mirrored in other regions that have lost grasslands to intensive agriculture and forestry. While demographic declines largely inform current conservation status of these species, we show that this is insufficient to capture declines in genetic diversity and resulting inbreeding, highlighting the acute need for genetic monitoring of wild insects to prevent extirpation and extinction. *Cyaniris semiargus*, a once widespread species in Sweden, now persists in segmented populations experiencing inbreeding depression and requiring prompt conservation action to reduce the risk of local extinction, providing a strong example of this.

Methods

Study System and Sampling

To assess changes in genetic diversity, differentiation, inbreeding, and genetic load, we selected three blue butterfly species (Polyommatinae) as focal species, *Polyommatus icarus*, *Plebejus argus*, and *Cyaniris semiargus* Figure 1A. These three species were selected as they vary in habitat specialization, being grassland generalist, heathland specialist, and grassland specialist, respectively, in order to assess how specialization may impact genetic decline. For these three species, we used population level genetic

data we previously generated (36) as our modern dataset. We selected pinned specimens from the entomological collections of the Biological Museum, Lund University (35) that corresponded to roughly the same geographic area as the modern samples for each species. These historical specimens were sampled between 1917-1956, during the early stages of the second wave of agricultural modernization in Sweden (29). For each historical locality, we selected 4-11 specimens sampled in the same year to estimate population level metrics. The historical and modern population level pairs were sampled in four broad geographic areas: I) Western and II) Eastern Skåne, III) Småland, and IV) Öland (Figure 1B), with historical localities ranging approximately 12-40km from their modern counterparts. This resulted in historical-modern population level pairs for three regions in *Po. icarus* (Western and Eastern Skåne and Öland), two regions in *Pl. argus* (Småland and Öland), and three regions in *Cy. semiargus* (Western and Eastern Skåne and Småland). While most regions consist of only one historical-modern population pair, we additionally compared a modern *Cy. semiargus* population in Southeastern Skåne to the historical Eastern Skåne population. We were unable to sample population level historical data for *Pl. argus* in Skåne, however we did sample one historical specimen each from Western and Eastern Skåne, which we include in individual level analyses, pairing them with the modern samples from Southwestern and Eastern Skåne, respectively.

To more broadly assess the variation in rates of genetic decline in Polyommatinae of differing conservation statuses, we sampled historical and modern individuals of seven additional species: *Agriades optilete, Aricia agestis, Celastrina argiolus, Polyommatus amandus, Phengaris alcon, Scolitantides orion,* and *Plebejus argyrognomon.* Modern specimens of *Ag. optilete, Ar. agestis, Ce. argiolus,* and *Po. amandus* were collected across the same geographic regions as the focal species in 2021 (Table S1). Pinned specimens to be used as modern samples of *Ph. alcon* and *S. orion,* collected in 2003 in Western Skåne and 2016 in Södermanland, respectively, were donated to this study by Håkan Elmqvist. Legs from a pinned speciemen of *Pl. argyrognomon*, collected in 2003 in Western Skåne, were donated by Göran Engqvist and used as the modern sample for this species. The historical samples for these eight species all were selected to be proximal to the modern specimen sampling locality with collection dates ranging

from 1932-1967, all provided as pinned specimens from the entomological collections of the Biological Museum, Lund University (35).

DNA Extraction and Sequencing

DNA from fresh specimens was extracted and sequenced following the methods in Nolen et al (36). We extracted DNA and prepared sequencing libraries from pinned museum specimens in a facility dedicated to historical DNA processing at Lund University, following the protocol described by Twort et al (65). Libraries prepared for pinned specimens were pooled into two equimolar pools containing 37-38 libraries each, sequencing each pool on a single NovaSeq 6000 S4 lane. DNA was extracted from the abdomens or legs of male specimens without homogenization to preserve anatomical structures. Abdomens were then stored in glycerol together with the original specimen.

Genomic Analyses

We performed the majority of our analyses using the PopGLen pipeline (66), a Snakemake (67) pipeline we have built that combines several genotype likelihood based population genomic analyses. Genotype likelihood based analyses use a probabilistic framework to account for the uncertainty that comes with low coverage sequencing data, reducing biases related to lower sequencing depth in our historical samples. We utilized genotype likelihood based analyses for all results, except for the estimation of inbreeding coefficients and genetic load, where the chosen methods required called genotypes.

Sequence Processing

We pre-processed both modern and historical raw sequencing data using fastp v0.23.4 (68), using default settings to trim low quality base pairs and poly-G tails from the ends of reads in modern samples and additionally collapsing overlapping read pairs in historical samples, where we discarded reads with less than 30bp overlap. This processing of historical samples discards short (<30bp) fragments that contain little data usable for unique mapping, as well as long fragments (>270bp) that are more likely to be modern contaminants.

We mapped the trimmed, paired modern reads separately per sequencing run to the respective species-specific reference genomes, or to the closest relative which an available chromosome level assembly (Table S12), using BWA mem v0.7.17 (69). We mapped the collapsed historical reads to the same reference genomes using BWA aln, which is the recommended algorithm for reads shorter than 70bp (70) using settings optimized for ancient/historical DNA (`-l 16500 -n 0.01 -o 2`) (71).

We merged mapped sequencing runs per sample using Samtools v1.17 (72) and removed PCR and optical duplicates using Picard v2.27 (73) with default settings except for an optical duplicate pixel distance of 2500 as recommended for patterned flow cell data. We removed PCR duplicates for our historical samples using dedup v0.12.8 (74), which identifies duplicates using both ends of the collapsed sequencing read.

We realigned around indels using the GATK IndelRealigner (75). As the primary tool we are using, ANGSD, counts overlapping reads twice (76), we additionally clipped overlapping read pairs in the modern samples using BamUtil v1.0.15 (77). We estimated post-mortem DNA damage in historical samples using DamageProfiler v1.1 (78).

Site and read filtering

We utilized a site based filtering scheme similar to that implemented in (79) in which we developed multiple independent sets of filtered sites, generating a global list of filtered sites from all analyses that excludes sites filtered by any of the sets. We performed this filtering for each species dataset separately.

We excluded sex linked chromosomes, mitochondria, and scaffolds less than 1 Mb in length. We excluded repeats identified by RepeatMasker v4.1.2 (80), using the reference specific repeat libraries provided by the Darwin Tree of Life Project (https://projects.ensembl.org/darwin-tree-of-life/). We estimated regions in the lower 1% and upper 99% of global sequencing depth separately across all samples, historical samples, and modern samples, excluding sites that appeared in any of the three sets. The number and proportion of sites passing each of these filters, as well as passing the

final intersected filter set, are reported for each species in Table S13. We estimated mean sequencing depth without filtering, as well as within the filtered site set, for each sample using ANGSD (Table S1). All subsequent analyses were performed on the species-specific filtered site sets.

Reference bias and post-mortem DNA damage

Due to DNA degradation, historical samples will have fragmented DNA with post-mortem damage that alters base composition (81). We investigated two potential methods to account for post-mortem DNA damage: I) recalibration of putatively damaged bases using MapDamage2 (39), and II) removal of transitions across the dataset, where most DNA damage is expected to occur (37, 38). To assess the performance of these methods, we compared the identity by state (IBS) similarity to the reference at filtered sites between these two correction methods and the uncorrected data (Figure S2). We estimated the identity by state similarity to the reference using ANGSD's `-doIBS 1` function with the `-doMajorMinor 4` and `-output01 1` options, which together sample a single base at each position, assigning 1 to positions that sample the reference base and 0 to positions sampling the non-reference. We calculated individual identity by state similarity to the reference by averaging these values, where a value of 1 indicates complete similarity to the reference and 0 indicates complete dissimilarity.

Historical samples without correction had less similarity to the reference than modern (Figure S2), which is expected for historical samples without substantial mapping bias due to drift from the sampling time of the historical samples and the modern reference as well as differences introduced by post-mortem DNA damage (82, 83), suggesting shorter fragment size does not introduce substantial reference bias. After MapDamage2 rescaling, historical samples showed higher identity by state similarity to the reference than modern samples in *Po. icarus* and *Pl. argus*. As removal of transitions did not introduce this reference bias, we proceeded using transition removal in all analyses to account for post-mortem DNA damage.

Genotype Likelihood Calculations

We estimated genotype likelihoods in ANGSD v0.940 (84) using the GATK model (`-GL 2`), using reads with a mapping quality greater than 30 (`-mapMapQ 30`) and base quality

greater than 20 (`-minQ 20`). We filtered our analyses to sites present in the species-specific filtered sites list using the `-sites` option.

Heterozygosity and genetic diversity metrics

We estimated individual genome-wide heterozygosity for all samples using the single sample site frequency spectrum (SFS) produced by realSFS, included with ANGSD. First, we generated a sample allele frequency (SAF) file using (`-doSaf 1`) for each sample, setting the ancestral state (`-anc`) to the reference sequence. We then generated a folded (`-fold 1`) SFS in realSFS using this SAF file and calculated heterozygosity as the second value (count of heterozygous sites) divided by the total sum of all values (count of total analyzed sites). To test for differences in mean individual heterozygosity across time periods, we performed an unequal variances *t*-test comparing all samples within each time category for each of the focal species.

For the three focal species with population level samples, we estimated nucleotide diversity, Watterson's θ, and Tajima's D per sampled population using thetaStat, included with ANGSD. As the estimates of these metrics, especially Watterson's θ and Tajima's D, can depend on sample size, we made our estimates using 100 subsamples of each population to four individuals. For each subsample, we estimated a SAF file in the same fashion as the heterozygosity estimates, additionally limited to sites for which three of the four subsampled individuals had data (`-minInd 3`). We then used realSFS to generate a folded SFS and thetaStat to estimate these three diversity metrics from the SAF file and SFS in 10kb sliding windows with a step size of 5kb, excluding windows with less than 1000 usable sites. The per site estimate of these three metrics was obtained for each window by dividing the window estimate by the number of usable sites (`nsites`). We report the median estimate across subsamples as the population estimate of each metric. To statistically assess differences between historical and modern populations, we performed a paired difference Wilcoxon signed-rank test each corresponding historical and modern subsamples, pairing estimates by genomic window. We estimated the effect size using the following equation:

$$\frac{Z}{\sqrt{N_{win}}}$$

where Z is the *Z*-score from the Wilcoxon signed-rank test and N_{win} is the number of paired windows. We considered modern populations to have significantly different estimates of nucleotide diversity, Watterson's θ, or Tajima's D if the distribution of effect sizes across all 100 subsample tests did not overlap 0.

Genetic Differentiation

We estimated genetic differentiation using pairwise population F_{ST} using realSFS. We generated population SAF files using the same parameters as for the genetic diversity metrics and generated a two dimensional folded SFS for each population pair using realSFS. We then used this SFS and the population SAF files to estimate a global estimate of F_{ST} using the Bhatia estimator (`-whichFst 1`), which is less sensitive to small or uneven sample sizes (85). Where reported, F_{ST} estimates refer to the weighted F_{ST}. To statistically assess differences in F_{ST} between modern and historical populations, we performed two tests: I) a paired *t*-test pairing corresponding population pairs in historical and modern population sets and II) an unequal variances unpaired *t*-test incorporating all possible population pairs in each set, comparing the historical to the modern population set.

Relatedness

As the analyses we utilize to assess population structure can be sensitive to the presence of close relatives in the dataset, we estimated pairwise relatedness between all samples within each species dataset. We utilized the IBSrelate SFS-based method (86), as implemented in NGSrelate (87), to estimate R0, R1, and KING-robust kinship coefficients (88) for all pairs of individuals in the dataset. For input, we generated a Beagle file using ANGSD for each focal species dataset (`-doGlf 2`), utilizing only positions where greater than 80% of the individuals had data, calling SNPs (`-SNP_pval 1e-6`) and assuming known major and minor alleles inferred from the genotype likelihoods (`-doMajorMinor 1 -doMaf 1`) (89, 90).

Population Structure

We explored population structure using principal component analysis (PCA) as implemented in PCAngsd v1.10 (91). As the population structure methods we use

assume independence of sites, we first estimated linkage disequilibrium for SNPs less than 50kb apart in the species dataset Beagle files using ngsLD v1.2.0 (92). We pruned SNPs using the recommended prune_graph tool (https://github.com/fgvieira/prune_graph; v0.3.2), assuming independence of SNPs >50kb apart and with a coefficient of correlation (r^2) < 0.1 and subset the Beagle file to include only pruned sites. We then removed one individual from each pair of third-degree or closer relatives in the dataset (expected KING-kinship coefficient >= 0.0625; Table S14) before running the analysis.

We formally tested for the presence of population structure using an admixture analysis for 1-10 ancestral cluster (K) using the pruned, relative removed Beagle file in NGSadmix v33 (93). We performed at least 20 replicate runs for each value of K, up to 100 total runs, stopping if the three highest likelihood replicates converged within 2 log-likelihood units of each other. The 'best-fit' value for K was then determined to be the highest K for which replicates met this convergence criteria, following Pečnerová et al (79). We further assessed the quality of the model fit for each value of K using evalAdmix v0.961 (94).

Genotype Calling

To estimate runs of homozygosity and genetic load in our three focal species, we utilized methods that require genotype calls. As genetic load estimates can be biased by variation in sequencing depth (14), we subsampled all samples to a mean 5X filtered sequencing depth using Samtools, excluding samples with a mean filtered sequencing depth below 5X from genotype call based analyses. We called genotypes per sample using BCFtools multi-allelic caller v1.19 (72). Calling was performed only for regions in our filtered sites file, using reads with a minimum mapping quality of 30 and bases with a minimum quality of 20. We set genotypes with a read depth <4 to missing. We additionally filtered heterozygous calls for allelic balance, setting heterozygous genotypes where one allele was supported by <20% of the reads to missing. We then merged the samples into a single BCF per species, filtering SNPs within 5bp of indels, removing indels, and including only biallelic SNPs that were segregating in the dataset.

Finally, we only included sites with called genotypes in 80% of samples and excluded all transition variants.

Runs of Homozygosity

We assessed rates of recent and background inbreeding by estimating the inbreeding coefficient F_{RoH}, the proportion of the autosomal genome existing in runs of homozygosity over a specified length, for each individual from the genotype calls. We incorporated runs of homozygosity >100kb into our estimates of F_{RoH}. We estimated runs of homozygosity using BCFtools/RoH v1.19 (95), setting a constant species-specific recombination rate (`-M`; estimated assuming 50 centimorgans per autosomal chromosome as in Mackintosh et al (21), estimates in Table S12) and running the analysis on genotype calls only, with the PL of unseen genotypes set to 30 (`-G30`). As we did not have sufficient samples to confidently estimate population allele frequencies, we used a default minor allele frequency of 0.4 (`--AF-dflt 0.4`). We additionally ignored homozygous reference positions (`--ignore-homref`), as including these can inflate estimates of F_{RoH} when using a default allele frequency based on our testing (Figure S9). We calculated F_{RoH} for each individual by dividing the total sum of runs of homozygosity greater than 100kb in length by the total length of the autosomes.

Genetic load

We estimated individual levels of genetic load from the genotype calls using two complementary methods, one targeting conserved regions of the genome (96) and the other utilizing gene annotations to infer functional effects (97). We filtered the input genotype calls for all genetic load analyses to include only positions with genotype calls for 80% of the individuals in both the historical and the modern subsets.

Genomic conservation based methods utilize multiple species alignments to determine genomic regions that are highly conserved across a taxonomic group, with deviations from the ancestral state being likely to be deleterious. To estimate to which extent the focal species had accumulated deleterious variants in conserved regions of the genome, we used the GenErode pipeline v0.6.0 (98) to estimate Genomic Evolutionary Rate Profiling (GERP) scores (99) across each of the three focal species genomes. The method implemented in this pipeline does not require a multi-species alignment, instead

fragmenting the outgroup genomes and mapping the fragments to the target to generate alignments which are then used to estimate scores. We used a dataset of 106 Lepidoptera chromosome level outgroup genomes (Table S15) to estimate the scores and ancestral states, using divergence times estimated with TimeTree 5 (100). We selected the highest 1% of GERP scores as the most conserved positions using the `get_gerp_score_percentile.py` script included with GenErode. We estimated the total relative genetic load at conserved sites for each individual by multiplying the derived allele count at each position by its GERP score, summing these values across the genome and dividing by the total derived allele count for that individual. We estimate realized relative genetic load by multiplying the derived allele count for homozygous derived genotypes by the GERP score, summing these values across the genome and dividing by the total derived allele count for that individual. While estimating realized load in this fashion neglects the realized effects of variants with partial dominance in heterozygous state (9), the majority of mildly and highly deleterious mutations are likely to be recessive (101) and realized only in homozygous state (82).

For the functional annotation based method, we used the annotations by the Darwin Tree of Life Project (https://projects.ensembl.org/darwin-tree-of-life/). We assigned impacts to each variant using Ensembl's Variant Effect Predictor (VEP) v112.0 (97). VEP categorizes variants into four classes: 'High', 'Moderate', 'Low', or 'Modifier', which largely correspond to loss of function, missense, synonymous, and intergenic variants. As variants often overlap multiple transcripts, multiple impacts will be assigned, so we required VEP to pick one effect per variant (`--flag_pick`), using the default selection order. After assignment, we estimated total and realized genetic load at high and moderate impact variants, treating the alternate allele as the putatively deleterious variant. We estimated total genetic load as the alternative allele count for the given impact category, divided by the total count of alternate alleles. We estimated realized genetic load as the alternative allele count for homozygous alternate positions for the given impact category, divided by the total count of alternate alleles.

Categorizing rates of genetic decline

To assess the changes in genetic diversity in a framework developed for conservation focused genetic monitoring, we used the indicator thresholds suggested by Andersson et al (15), which are based upon indicators applied for national use in Sweden (102). Using these thresholds, genetic decline within populations is measured as the amount of genetic diversity retained over a period of 100 years, assuming a constant rate of change. Three threat categories are suggested: retention >=95% is considered 'Acceptable', 75-94% as 'Warning', and <75% as 'Alarm'. As different population genetic estimates of genetic diversity are influenced by different components of genetic diversity, such as rare and common variants, this metric can be assessed for each estimate separately.

We estimated the predicted retention of genetic diversity over 100 years for each population using individual heterozygosity, nucleotide diversity, and Watterson's θ. Genetic diversity retention per year was estimated using the following equation:

$$e^{\frac{ln(H_{mod}/H_{hist})}{Y_{mod}-Y_{hist}}}$$

where H is the estimate of genetic diversity for a given sample/population and Y is the sampling year for that sample/population. As different populations had different sample sizes, we used repeated subsamples to generate estimates of decline. For individual heterozygosity, we performed all pairwise comparisons of historical and modern individual estimates of heterozygosity within corresponding historical-modern sample pairs, generating a single estimate for species with only one specimen per time period and a range for ones with more (see Figure 4). For nucleotide diversity and Watterson's θ, we utilized the previously generated 100 subsamples (N=4) for each population, estimating H_{mod}/H_{hist} for paired historical and modern populations for each subsample, utilizing the median value of H_{mod}/H_{hist} across subsamples to calculate the predicted retention.

Acknowledgements

We would like to thank Melina Eberhagen, Amanda Görnerup, Kajsa Svensson, Aske Brydegaard Runemark, and Mikkel Brydegaard for assistance with collecting butterflies, Håkan Elmqvist for providing pinned specimens of *Ph. alcon* and *S. orion*, Göran Engqvist for providing tissue from the pinned specimen of *Pl. argyrognomon*, Emma Kärrnäs and Isolde van Riemsdijk for assistance with DNA extraction of samples, Jadranka Rota for assistance with the entomological collections of the Biological Museum, Lund University (https://doi.org/10.15468/dahk2a), Verena Kutschera and the Swedish Bioinformatics Advisory Program for advice regarding the bioinformatic analyses, Anna Penna for comments on the manuscript, and Isolde van Riemsdijk, Rachel Steward, Kalle Tunström, Simon Jacobsen Ellestrand, and Magne Friberg for helpful discussions regarding the study species, methods and interpretations. The computations were enabled by resources provided by the National Academic Infrastructure for Supercomputing in Sweden (NAISS) and the Swedish National Infrastructure for Computing (SNIC) at UPPMAX partially funded by the Swedish Research Council through grant agreements no. 2022-06725 and no. 2018-05973. This work was supported by grants from the Strategic Research Area “Biodiversity and Ecosystem services in a Changing Climate” (BECC), funded by the Swedish government, the Foundation Oscar och Lili Lamms Minne, the Jörgen Lindström’s Foundation, and the Swedish Research Council for Sustainable Development (grant 2021-01163).

Data Availability Statement

The genetic data that support these findings will be made available upon publication at NCBI in BioProjects PRJNA1068054 (focal species, modern) & PRJNA1168917 (focal species, historical; additional species). The main population genomic pipeline is available at https://doi.org/10.5281/zenodo.13785563. Workflow configurations, extensions, and resources specific to this study are available at https://github.com/zjnolen/polyommatini-temporal-genomics.

Author Contributions

Zachary J. Nolen: Conceptualization, Methodology, Formal analysis, Investigation (Lead), Data curation, Writing – original draft, Visualization, Funding acquisition. **Patrycja Jamelska**: Investigation (Supporting), Writing - review & editing. **Ana Sofía Torres Lara**: Investigation (Supporting), Writing - review & editing. **Niklas Wahlberg:** Methodology, Writing – review & editing, Supervision. **Anna Runemark:** Conceptualization, Methodology, Writing – review & editing, Supervision, Funding acquisition.

References

1. D. L. Wagner, E. M. Grames, M. L. Forister, M. R. Berenbaum, D. Stopak, Insect decline in the anthropocene: Death by a thousand cuts. *Proceedings of the National Academy of Sciences* **118**, e2023989118 (2021).

2. R. van Klink, *et al.*, Meta-analysis reveals declines in terrestrial but increases in freshwater insect abundances. *Science* **368**, 417–420 (2020).

3. R. Dirzo, *et al.*, Defaunation in the Anthropocene. *Science* **345**, 401–406 (2014).

4. C. A. Halsch, *et al.*, Insects and recent climate change. *Proceedings of the National Academy of Sciences* **118**, e2002543117 (2021).

5. P. H. Raven, D. L. Wagner, Agricultural intensification and climate change are rapidly decreasing insect biodiversity. *Proceedings of the National Academy of Sciences* **118**, e2002548117 (2021).

6. S. Seibold, *et al.*, Arthropod decline in grasslands and forests is associated with landscape-level drivers. *Nature* **574**, 671–674 (2019).

7. D. H. Boyes, D. M. Evans, R. Fox, M. S. Parsons, M. J. O. Pocock, Is light pollution driving moth population declines? A review of causal mechanisms across the life cycle. *Insect Conservation and Diversity* **14**, 167–187 (2021).

8. J. R. Shipley, *et al.*, Agricultural practices and biodiversity: Conservation policies for semi-natural grasslands in europe. *Current Biology* **34**, R753–R761 (2024).

9. G. Bertorelle, *et al.*, Genetic load: genomic estimates and applications in non-model animals. *Nature Reviews Genetics* **23**, 492–503 (2022).

10. M. Lynch, W. Gabriel, Mutation Load and the Survival of Small Populations. *Evolution* **44**, 1725–1737 (1990).

11. D. L. Gilroy, K. P. Phillips, D. S. Richardson, C. van Oosterhout, Toll-like receptor variation in the bottlenecked population of the Seychelles warbler: computer simulations see the ’ghost of selection past’ and quantify the ’drift debt’. *Journal of Evolutionary Biology* **30**, 1276–1287 (2017).

12. A. V. Pinto, B. Hansson, I. Patramanis, H. E. Morales, C. van Oosterhout, The impact of habitat loss and population fragmentation on genomic erosion. *Conservation Genetics* **25**, 49–57 (2024).

13. H. A. Jackson, *et al.*, Genomic erosion in a demographically recovered bird species during conservation rescue. *Conservation Biology* **36**, e13918 (2022).

14. M. Dehasque, *et al.*, Temporal dynamics of woolly mammoth genome erosion prior to extinction. *Cell* **187**, 3531–3540.e13 (2024).

15. A. Andersson, S. Karlsson, N. Ryman, L. Laikre, Monitoring genetic diversity with new indicators applied to an alpine freshwater top predator. *Molecular Ecology* **31**, 6422–6439 (2022).

16. D. O'Brien, *et al.*, Bringing together approaches to reporting on within species genetic diversity. *Journal of Applied Ecology* **59**, 2227–2233 (2022).

17. K. Theissinger, *et al.*, How genomics can help biodiversity conservation. *Trends in Genetics* **39**, 545–559 (2023).

18. D. Díez-del-Molino, F. Sánchez-Barreiro, I. Barnes, M. T. P. Gilbert, L. Dalén, Quantifying temporal genomic erosion in endangered species. *Trends in Ecology & Evolution* **33**, 176–185 (2018).

19. H. Ellegren, N. Galtier, Determinants of genetic diversity. *Nature Reviews Genetics* **17**, 422–433 (2016).

20. J. Romiguier, *et al.*, Comparative population genomics in animals uncovers the determinants of genetic diversity. *Nature* **515**, 261–263 (2014).

21. A. Mackintosh, *et al.*, The determinants of genetic diversity in butterflies. *Nature Communications* **10**, 3466 (2019).

22. G. Hewitt, The genetic legacy of the Quaternary ice ages. *Nature* **405**, 907–913 (2000).

23. J. A. Robinson, *et al.*, Genomic flatlining in the endangered island fox. *Current Biology* **26**, 1183–1189 (2016).

24. J. A. Robinson, *et al.*, The critically endangered vaquita is not doomed to extinction by inbreeding depression. *Science* **376**, 635–639 (2022).

25. M. F. DiLeo, A. Nair, M. Kardos, A. Husby, M. Saastamoinen, Demography and environment modulate the effects of genetic diversity on extinction risk in a butterfly metapopulation. *Proceedings of the National Academy of Sciences* **121**, e2309455121 (2024).

26. N. Dussex, H. E. Morales, C. Grossen, L. Dalén, C. van Oosterhout, Purging and accumulation of genetic load in conservation. *Trends in Ecology & Evolution* **38**, 961–969 (2023).

27. M. K. Schwartz, G. Luikart, R. S. Waples, Genetic monitoring as a promising tool for conservation and management. *Trends in Ecology & Evolution* **22**, 25–33 (2007).

28. S. Hoban, *et al.*, Effective population size remains a suitable, pragmatic indicator of genetic diversity for all species, including forest trees. *Biological Conservation* **253**, 108906 (2021).

29. M. Ihse, Swedish agricultural landscapes patterns and changes during the last 50 years, studied by aerial photos. *Landscape and Urban Planning* **31**, 21–37 (1995).

30. R. Lindborg, O. Eriksson, Historical Landscape Connectivity Affects Present Plant Species Diversity. *Ecology* **85**, 1840–1845 (2004).

31. D. L. Wagner, R. Fox, D. M. Salcido, L. A. Dyer, A window to the world of global insect declines: Moth biodiversity trends are complex and heterogeneous. *Proceedings of the National Academy of Sciences* **118**, e2002549117 (2021).

32. M. S. Warren, *et al.*, The decline of butterflies in europe: Problems, significance, and possible solutions. *Proceedings of the National Academy of Sciences* **118**, e2002551117 (2021).

33. J. C. Habel, *et al.*, Butterfly community shifts over two centuries. *Conservation Biology* **30**, 754–762 (2016).

34. SLU Artdatabanken, *Rödlistade arter i Sverige 2020* (SLU, 2020).

35. C. Fägerström, Lund University Biological Museum - Insect collections Inventory. (2024). https://doi.org/10.15468/dahk2a.

36. Z. J. Nolen, M. Rundlöf, A. Runemark, Species-specific erosion of genetic diversity in grassland butterflies depends on landscape land cover. *Biological Conservation* **296**, 110694 (2024).

37. M. T. P. Gilbert, *et al.*, Recharacterization of ancient DNA miscoding lesions: Insights in the era of sequencing-by-synthesis. *Nucleic Acids Research* **35**, 1–10 (2007).

38. M. Stiller, *et al.*, Patterns of nucleotide misincorporations during enzymatic amplification and direct large-scale sequencing of ancient DNA. *Proceedings of the National Academy of Sciences* **103**, 13578–13584 (2006).

39. H. Jónsson, A. Ginolhac, M. Schubert, P. L. F. Johnson, L. Orlando, mapDamage2.0: Fast approximate bayesian estimates of ancient DNA damage parameters. *Bioinformatics* **29**, 1682–1684 (2013).

40. P. W. Hedrick, *Genetics of Populations* (Jones & Bartlett Publishers, 2009).

41. R. McQuillan, *et al.*, Runs of homozygosity in european populations. *The American Journal of Human Genetics* **83**, 359–372 (2008).

42. E. A. Thompson, Identity by descent: Variation in meiosis, across genomes, and in populations. *Genetics* **194**, 301–326 (2013).

43. S. Glémin, How are deleterious mutations purged? Drift versus nonrandom mating. *Evolution* **57**, 2678–2687 (2003).

44. SLU Artdatabanken, Artfakta: kronärtsblåvinge (Plebejus argyrognomon).

45. J. C. Habel, M. J. Samways, T. Schmitt, Mitigating the precipitous decline of terrestrial European insects: Requirements for a new strategy. *Biodiversity and Conservation* **28**, 1343–1360 (2019).

46. E. L. Landguth, *et al.*, Quantifying the lag time to detect barriers in landscape genetics. *Molecular Ecology* **19**, 4179–4191 (2010).

47. C. W. Epps, N. Keyghobadi, Landscape genetics in a changing world: disentangling historical and contemporary influences and inferring change. *Molecular Ecology* **24**, 6021–6040 (2015).

48. W. H. Lowe, F. W. Allendorf, What can genetics tell us about population connectivity? *Molecular Ecology* **19**, 3038–3051 (2010).

49. P. W. Hedrick, J. R. Adams, J. A. Vucetich, Reevaluating and Broadening the Definition of Genetic Rescue. *Conservation Biology* **25**, 1069–1070 (2011).

50. P. W. Hedrick, A. Garcia-Dorado, Understanding inbreeding depression, purging, and genetic rescue. *Trends in Ecology & Evolution* **31**, 940–952 (2016).

51. D. A. Bell, *et al.*, The Exciting Potential and Remaining Uncertainties of Genetic Rescue. *Trends in Ecology & Evolution* **34**, 1070–1079 (2019).

52. R. Lande, Risk of population extinction from fixation of new deleterious mutations. *Evolution* **48**, 1460–1469 (1994).

53. S. Mathur, J. A. DeWoody, Genetic load has potential in large populations but is realized in small inbred populations. *Evolutionary Applications* **14**, 1540–1557 (2021).

54. I. Saccheri, *et al.*, Inbreeding and extinction in a butterfly metapopulation. *Nature* **392**, 491–494 (1998).

55. C. D. Huber, B. Y. Kim, K. E. Lohmueller, Population genetic models of GERP scores suggest pervasive turnover of constrained sites across mammalian evolution. *PLOS Genetics* **16**, e1008827 (2020).

56. C. C. Kyriazis, J. A. Robinson, K. E. Lohmueller, Using computational simulations to model deleterious variation and genetic load in natural populations. *The American Naturalist* **202**, 737–752 (2023).

57. N. Dussex, *et al.*, Population genomics of the critically endangered kākāpō. *Cell Genomics* **1**, 100002 (2021).

58. T. van der Valk, D. Díez-del-Molino, T. Marques-Bonet, K. Guschanski, L. Dalén, Historical Genomes Reveal the Genomic Consequences of Recent Population Decline in Eastern Gorillas. *Current Biology* **29**, 165–170.e6 (2019).

59. J. von Seth, *et al.*, Genomic insights into the conservation status of the world's last remaining Sumatran rhinoceros populations. *Nature Communications* **12**, 2393 (2021).

60. C. Bortoluzzi, *et al.*, Lepidoptera genomics based on 88 chromosomal reference sequences informs population genetic parameters for conservation. *bioRxiv* (2023). https://doi.org/10.1101/2023.04.14.536868.

61. L. B. Pettersson, H. Arnberg, *Svensk dagfjärilsövervakning, årsrapport för 2023* (Biologiska institutionen, Lunds universitet, 2024).

62. S. Hoban, *et al.*, Genetic diversity targets and indicators in the CBD post-2020 Global Biodiversity Framework must be improved. *Biological Conservation* **248**, 108654 (2020).

63. L. Laikre, *et al.*, Post-2020 goals overlook genetic diversity. *Science* **367**, 1083–1085 (2020).

64. G. Formenti, *et al.*, The era of reference genomes in conservation genomics. *Trends in Ecology & Evolution* **37**, 197–202 (2022).

65. V. G. Twort, J. Minet, C. W. Wheat, N. Wahlberg, Museomics of a rare taxon: placing Whalleyanidae in the Lepidoptera Tree of Life. *Systematic Entomology* **46**, 926–937 (2021).

66. Z. J. Nolen, Zjnolen/PopGLen: V0.3.0. (2024). https://doi.org/10.5281/zenodo.13785563. Deposited September 2024.

67. F. Mölder, *et al.*, Sustainable data analysis with snakemake [version 2; peer review: 2 approved]. *F1000Research* **10** (2021).

68. S. Chen, Y. Zhou, Y. Chen, J. Gu, Fastp: An ultra-fast all-in-one FASTQ preprocessor. *Bioinformatics* **34**, i884–i890 (2018).

69. H. Li, Aligning sequence reads, clone sequences and assembly contigs with BWA-MEM. (2013). https://doi.org/10.48550/arXiv.1303.3997.

70. H. Li, R. Durbin, Fast and accurate long-read alignment with BurrowsWheeler transform. *Bioinformatics* **26**, 589–595 (2010).

71. E. Palkopoulou, *et al.*, Complete genomes reveal signatures of demographic and genetic declines in the woolly mammoth. *Current biology: CB* **25**, 1395–1400 (2015).

72. P. Danecek, *et al.*, Twelve years of SAMtools and BCFtools. *GigaScience* **10** (2021).

73. Picard toolkit. *Broad Institute, GitHub Repository* (2019). Deposited 2019.

74. A. Peltzer, *et al.*, EAGER: efficient ancient genome reconstruction. *Genome Biology* **17**, 1–14 (2016).

75. G. A. van der Auwera, B. D. O'Connor, *Genomics in the Cloud: Using Docker, GATK, and WDL in Terra* (O'Reilly Media, Inc., 2020).

76. R. N. Lou, A. Jacobs, A. P. Wilder, N. O. Therkildsen, A beginner's guide to low-coverage whole genome sequencing for population genomics. *Molecular Ecology* **30**, 5966–5993 (2021).

77. G. Jun, M. K. Wing, G. R. Abecasis, H. M. Kang, An efficient and scalable analysis framework for variant extraction and refinement from population-scale DNA sequence data. *Genome Research* **25**, 918–925 (2015).

78. J. Neukamm, A. Peltzer, K. Nieselt, DamageProfiler: Fast damage pattern calculation for ancient DNA. *Bioinformatics* **37**, 3652–3653 (2021).

79. P. Pečnerová, *et al.*, High genetic diversity and low differentiation reflect the ecological versatility of the African leopard. *Current Biology* **31**, 1862–1871.e5 (2021).

80. A. F. A. Smit, R. Hubley, P. Green, RepeatMasker open-4.0. (2013). Deposited 2013.

81. S. Sawyer, J. Krause, K. Guschanski, V. Savolainen, S. Pääbo, Temporal Patterns of Nucleotide Misincorporations and DNA Fragmentation in Ancient DNA. *PLOS ONE* **7**, e34131 (2012).

82. G. Femerling, *et al.*, Genetic Load and Adaptive Potential of a Recovered Avian Species that Narrowly Avoided Extinction. *Molecular Biology and Evolution* **40**, msad256 (2023).

83. S. Gopalakrishnan, *et al.*, The population genomic legacy of the second plague pandemic. *Current Biology* **32**, 4743–4751.e6 (2022).

84. T. S. Korneliussen, A. Albrechtsen, R. Nielsen, ANGSD: Analysis of Next Generation Sequencing Data. *BMC Bioinformatics* **15**, 1–13 (2014).

85. G. Bhatia, N. Patterson, S. Sankararaman, A. L. Price, Estimating and interpreting FST: The impact of rare variants. *Genome Research* **23**, 1514–1521 (2013).

86. R. K. Waples, A. Albrechtsen, I. Moltke, Allele frequency-free inference of close familial relationships from genotypes or low-depth sequencing data. *Molecular Ecology* **28**, 35–48 (2019).

87. K. Hanghøj, I. Moltke, P. A. Andersen, A. Manica, T. S. Korneliussen, Fast and accurate relatedness estimation from high-throughput sequencing data in the presence of inbreeding. *GigaScience* **8**, giz034 (2019).

88. A. Manichaikul, *et al.*, Robust relationship inference in genome-wide association studies. *Bioinformatics* **26**, 2867–2873 (2010).

89. L. Skotte, T. S. Korneliussen, A. Albrechtsen, Association testing for next-generation sequencing data using score statistics. *Genetic Epidemiology* **36**, 430437 (2012).

90. S. Y. Kim, *et al.*, Estimation of allele frequency and association mapping using next-generation sequencing data. *BMC Bioinformatics* **12**, 231 (2011).

91. J. Meisner, A. Albrechtsen, Inferring population structure and admixture proportions in low-depth NGS data. *Genetics* **210**, 719–731 (2018).

92. E. A. Fox, A. E. Wright, M. Fumagalli, F. G. Vieira, ngsLD: Evaluating linkage disequilibrium using genotype likelihoods. *Bioinformatics* **35**, 3855–3856 (2019).

93. L. Skotte, T. S. Korneliussen, A. Albrechtsen, Estimating individual admixture proportions from next generation sequencing data. *Genetics* **195**, 693–702 (2013).

94. G. Garcia-Erill, A. Albrechtsen, Evaluation of model fit of inferred admixture proportions. *Molecular Ecology Resources* **20**, 936–949 (2020).

95. V. Narasimhan, *et al.*, BCFtools/RoH: A hidden markov model approach for detecting autozygosity from next-generation sequencing data. *Bioinformatics* **32**, 1749–1751 (2016).

96. E. V. Davydov, *et al.*, Identifying a High Fraction of the Human Genome to be under Selective Constraint Using GERP++. *PLOS Computational Biology* **6**, e1001025 (2010).

97. W. McLaren, *et al.*, The Ensembl Variant Effect Predictor. *Genome Biology* **17**, 122 (2016).

98. V. E. Kutschera, *et al.*, GenErode: a bioinformatics pipeline to investigate genome erosion in endangered and extinct species. *BMC Bioinformatics* **23**, 1–17 (2022).

99. G. M. Cooper, *et al.*, Distribution and intensity of constraint in mammalian genomic sequence. *Genome Research* **15**, 901–913 (2005).

100. S. Kumar, *et al.*, TimeTree 5: An expanded resource for species divergence times. *Molecular Biology and Evolution* **39**, msac174 (2022).

101. D. Charlesworth, J. H. Willis, The genetics of inbreeding depression. *Nature Reviews Genetics* **10**, 783–796 (2009).

102. K. Johannesson, L. Laikre, Monitoring of genetic diversity in environmental monitoring [in swedish]. *Report to the Swedish Agency for Marine and Water Management (dnr. HaV 3642-2018, 3643-2018)* (2020).

Figure Captions

Figure 1. Sampling design and changes in genetic diversity, differentiation, and inbreeding in the focal species. (A) Images of the three focal species. (B) Map of the sampling area in southern Sweden, sampling locations are approximate. Circles represent areas with modern samples in at least one of the species and triangles represent areas with historical samples, see Table S1 for complete sampling information. (C) Change in individual heterozygosity over time, measured as heterozygous sites per 1000bp, excluding transitions. Each point represents an individual sample, grouped into historical and modern samples per species. Coloring refers to sampling region and corresponds to the map in panel B. (D) Change in inbreeding coefficients over time, estimated using runs of homozygosity larger than 100kb (F_{RoH}). (E) Change in pairwise population genetic differentiation, F_{ST} over time between equivalent comparisons in each time period. Color of the points and line refer to the geographic distance between populations. Populations with no connecting line refer to pairs of modern sample populations that have no comparable historic pair. In C & D, results of unequal variance t-tests between historical and modern samples for each species is shown using the following scale, where panels without * are not significant ($P > 0.05$): * $P <= 0.05$, ** $P <= 0.01$, *** $P <= 0.001$, **** $P <= 0.0001$. Statistical assessment of genetic differentiation is not shown, as it could not be assessed for all three species (Table S7).

Figure 2. Population structure of the focal species. (A) Principal Component Analysis (PCA) of the three focal species. Shapes refer to sampling period, with each circle representing a modern and each triangle a historical individual, with colors corresponding to the sampling locations in Figure 1B. Percentages on each axis refer to the proportion of total variance explained by the component. (B) Best fit admixture analyses for the three focal species. Each bar represents an individual and each color one of K genetic clusters. Each bar is colored in proportion to the probability of the individual belonging to each cluster.

Figure 3. Changes in genetic load of the focal species (A) Individual inbreeding coefficients (F_{RoH}) partitioned by *RoH* size class. Longer *RoH* indicate more recent common ancestry of the identical haplotypes. (B) Total genetic load measured for conserved regions, high impact variants, and moderate impact variants. Total genetic load is measured for conserved region as the derived allele counts scaled by their genomic conservation (GERP) scores per 1000 conserved derived alleles. For high and moderate impact variants, total load is measured as alternate allele counts for the given impact category per 1000 alternate alleles. (C) Realized genetic load measured for the same three variant categories. Realized genetic load is measured for conserved region as the derived homozygous allele counts scaled by their conservation (GERP) scores per 1000 conserved derived alleles. For high and moderate impact variants, realized

load is measured as alternate allele counts in homozygous state for the given impact category per 1000 alternate alleles. In B & C, results of unequal variance t-tests between historical and modern samples are shown in each panel, where panels without * are not significant ($P > 0.05$): * $P <= 0.05$, ** $P <= 0.01$, *** $P <= 0.001$, **** $P <= 0.0001$.

Figure 4. Changes in heterozygosity predicted over 100 years based on the rate of change estimated from modern and historical samples for each of 11 species. Species are grouped by conservation status, which follows the species name on the x-axis. Background coloration refers to the three genetic decline thresholds outlined by Andersson et al (15), where a retention of >=95% over 100 year is considered 'acceptable' (green), a retention of 75-94% as 'warning' (yellow), and a retention of <75% as 'alarm' (red). Points represent mean estimates for change in heterozygosity across all sample pairs for a species. Species with bars have more than one possible sample pair, with error bars illustrating the spread of estimates across all sample pairs. Species with a * next to their species name on the x-axis have been mapped to a related species' reference genome as they lack a species-specific genome (Table S12).

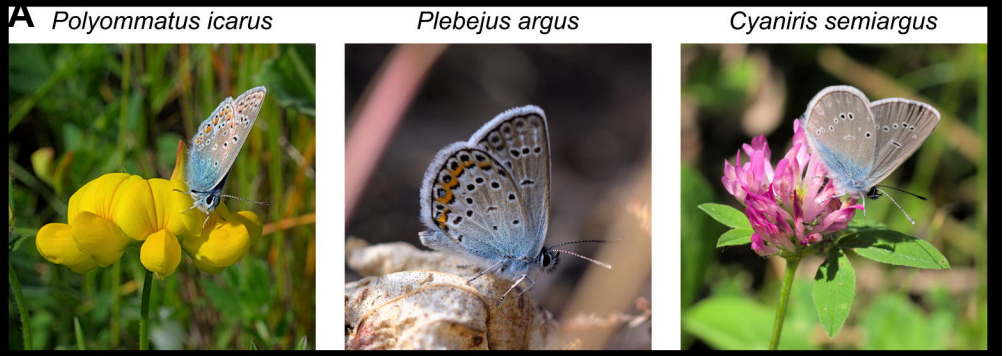
A
Polyommatus icarus
Plebejus argus
Cyaniris semiargus

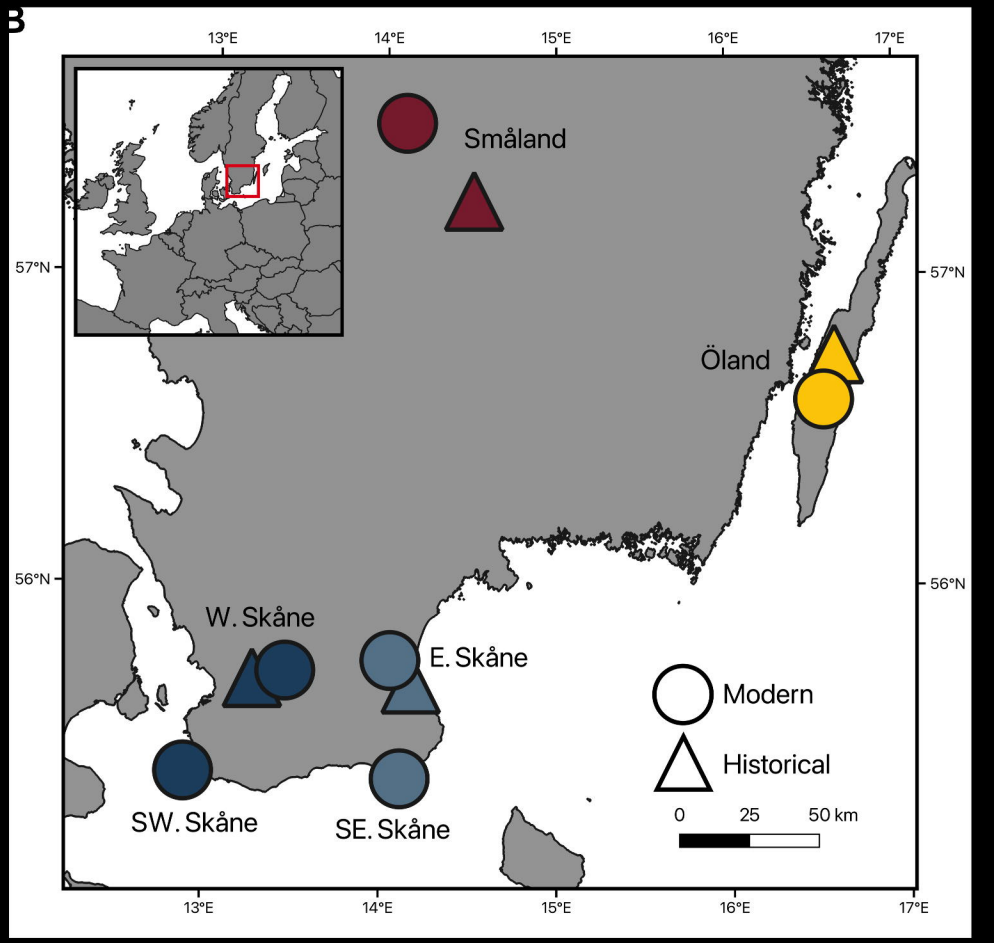
B
13°E
14°E
15°E
16°E
17°E
57°N
56°N
Småland
Öland
W. Skåne
E. Skåne
SW. Skåne
SE. Skåne
Modern
Historical
0
25
50 km

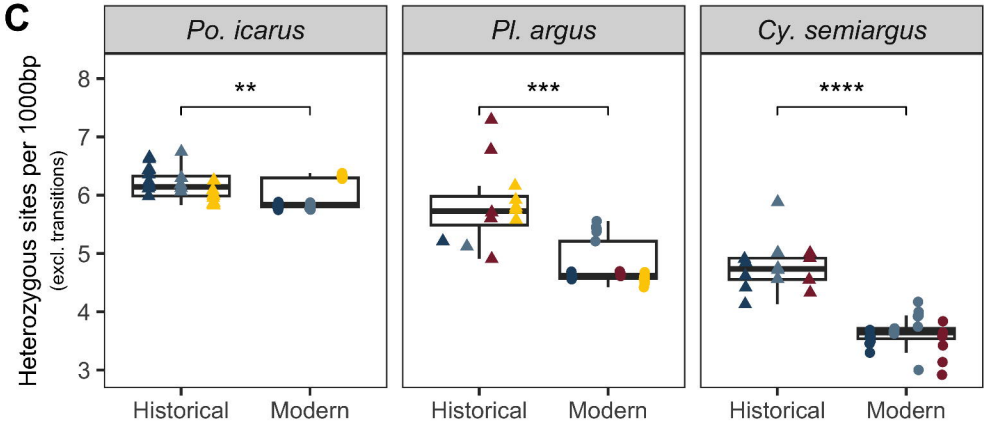
C
Po. icarus
Pl. argus
Cy. semiargus
Heterozygous sites per 1000bp
(excl. transitions)
**
***
****
Historical
Modern

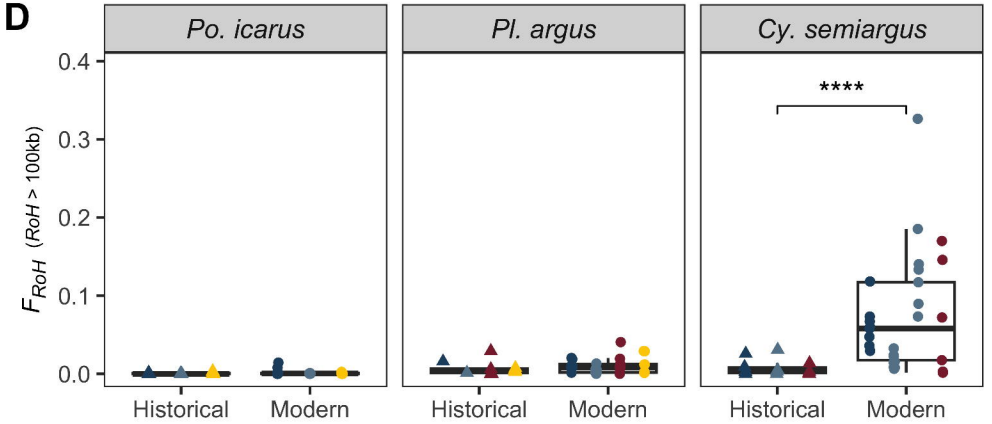
D
Po. icarus
Pl. argus
Cy. semiargus
F_{RoH} (RoH > 100kb)
****
Historical
Modern

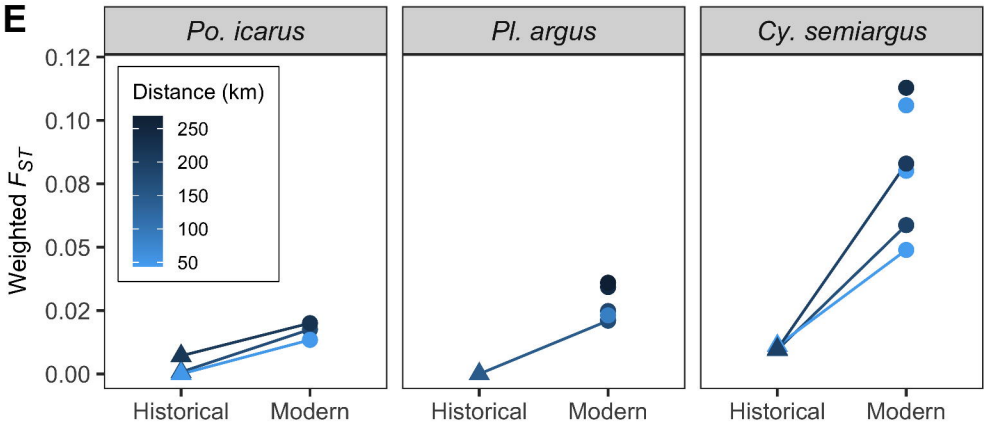
E
Po. icarus
Pl. argus
Cy. semiargus
Weighted F_{ST}
Distance (km)
250
200
150
100
50
Historical
Modern

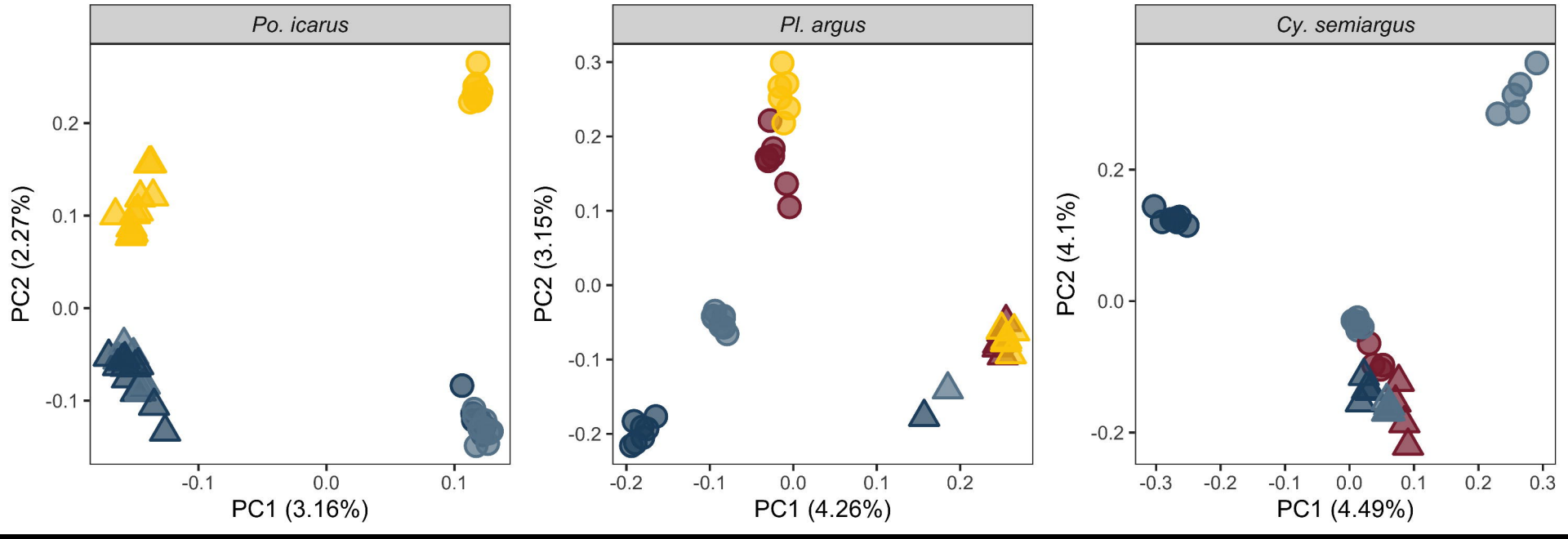
Po. icarus
Pl. argus
Cy. semiargus
PC2 (2.27%)
PC1 (3.16%)
PC2 (3.15%)
PC1 (4.26%)
PC2 (4.1%)
PC1 (4.49%)

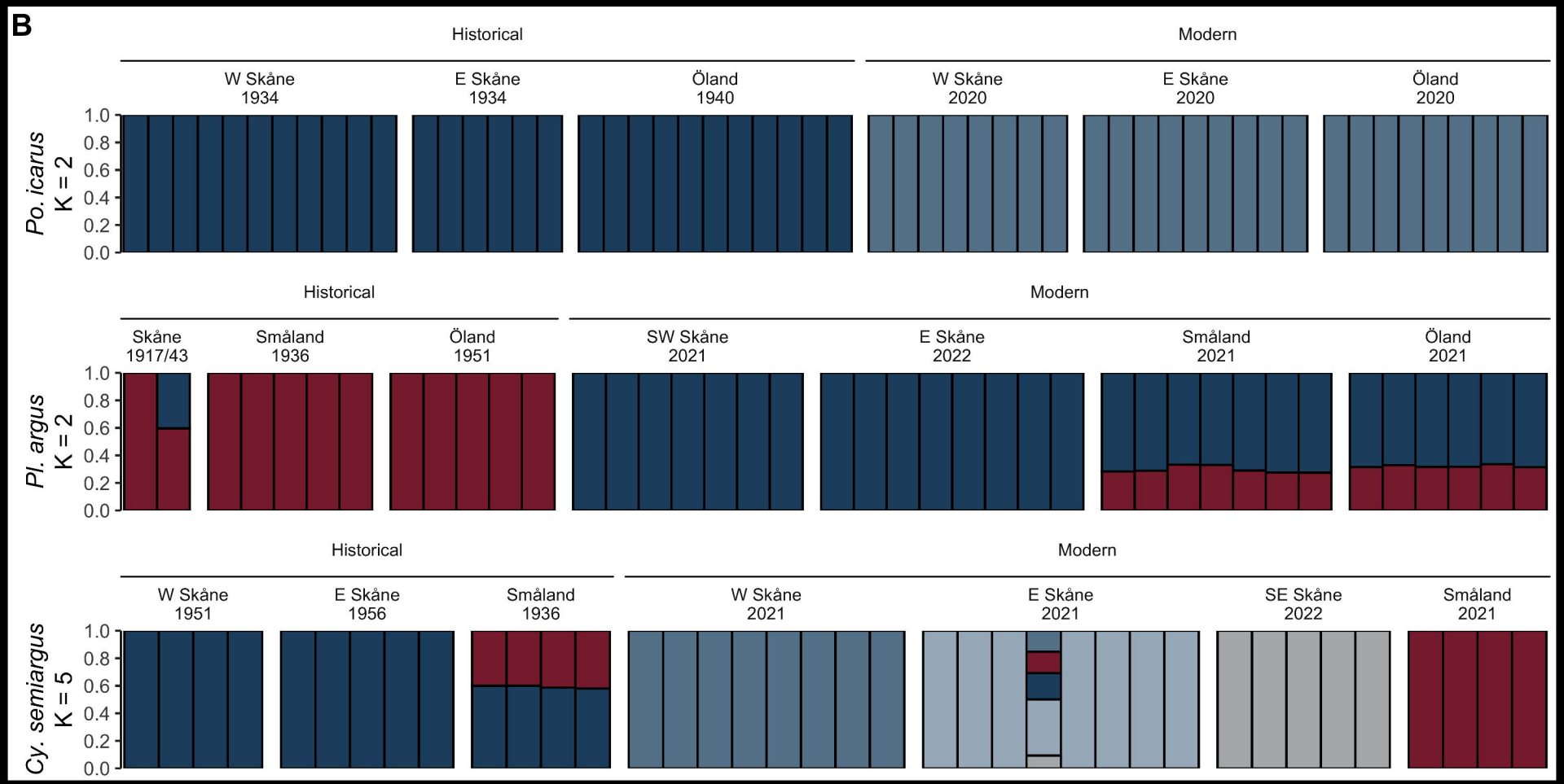
B
Historical
Modern
W Skåne 1934
E Skåne 1934
Öland 1940
W Skåne 2020
E Skåne 2020
Öland 2020
Po. icarus K = 2
Skåne 1917/43
Småland 1936
Öland 1951
SW Skåne 2021
E Skåne 2022
Småland 2021
Öland 2021
Pl. argus K = 2
W Skåne 1951
E Skåne 1956
Småland 1936
W Skåne 2021
E Skåne 2021
SE Skåne 2022
Småland 2021
Cy. semiargus K = 5

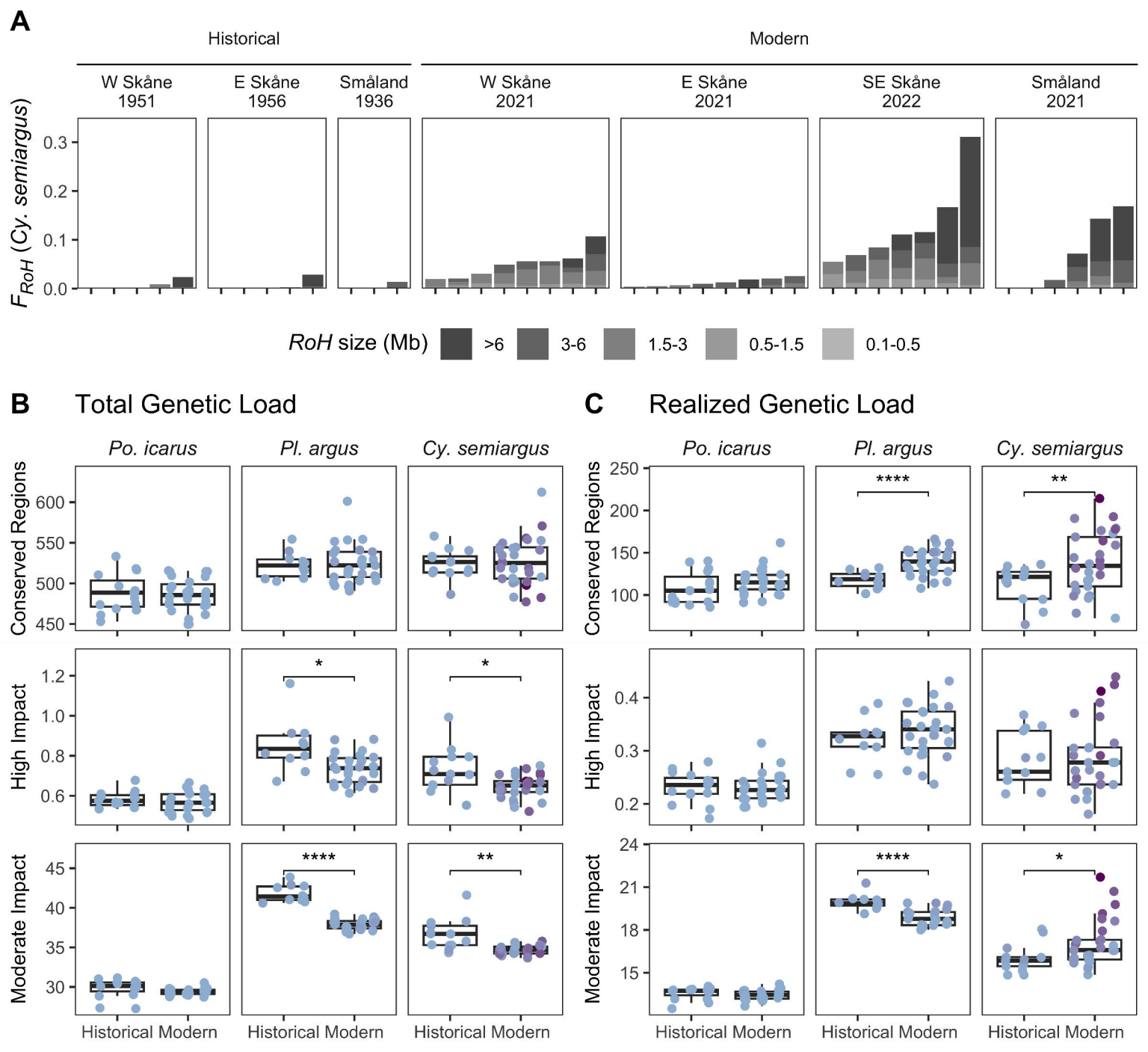
A
Historical
Modern
W Skåne 1951
E Skåne 1956
Småland 1936
W Skåne 2021
E Skåne 2021
SE Skåne 2022
Småland 2021
F_RoH (Cy. semiargus)
0.0
0.1
0.2
0.3
RoH size (Mb)
>6
3-6
1.5-3
0.5-1.5
0.1-0.5
B Total Genetic Load
C Realized Genetic Load
Po. icarus
Pl. argus
Cy. semiargus
Conserved Regions
High Impact
Moderate Impact
Historical
Modern
F_RoH
0.0
0.1
0.2
0.3

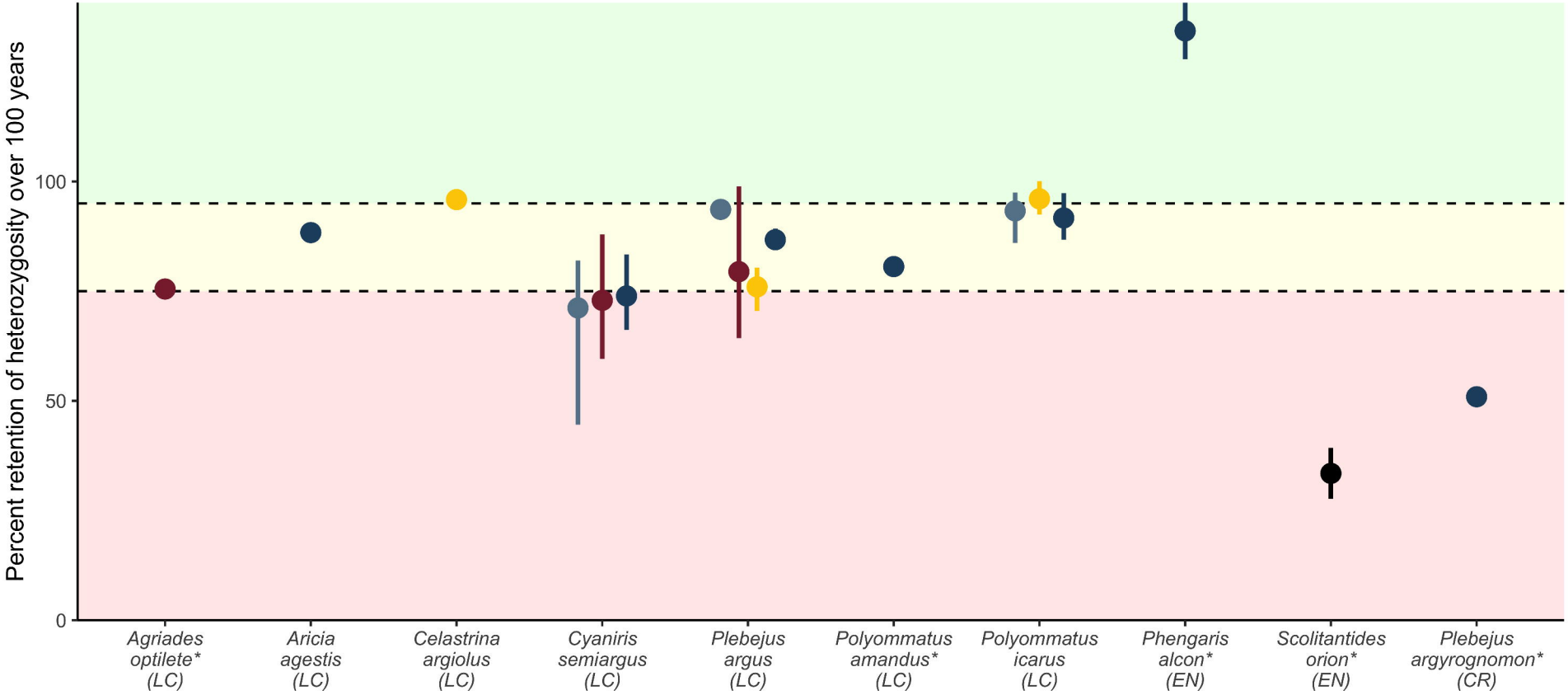
Percent retention of heterozygosity over 100 years
100
50
0
Agriades optilete* (LC)
Aricia agestis (LC)
Celastrina argiolus (LC)
Cyaniris semiargus (LC)
Plebejus argus (LC)
Polyommatus amandus* (LC)
Polyommatus icarus (LC)
Phengaris alcon* (EN)
Scolitantides orion* (EN)
Plebejus argyrognomon* (CR)